A General Reliability Model for Ni-BaTiO₃-Based Multilayer Ceramic Capacitors

Donhang (David) Liu

AS and D, Inc.
7515 Mission Drive, Suite 200, Seabrook, MD 20706
Work performed for NASA Goddard Space Flight Center
8800 Greenbelt Road, Greenbelt, Maryland 20771, USA
Donhang.liu-1@nasa.gov

Abstract

The evaluation for potential space project applications of multilayer ceramic capacitors (MLCCs) with Ni electrode and BaTiO₃ dielectric material requires an in-depth understanding of the MLCCs' reliability. A general reliability model for Ni-BaTiO₃ MLCCs is developed and discussed in this paper. The model consists of three parts: a statistical distribution; an acceleration function that describes how a capacitor's reliability life responds to external stresses; and an empirical function that defines the contribution of the structural and constructional characteristics of a multilayer capacitor device, such as the number of dielectric layers N, dielectric thickness d, average grain size $\bar{r}$, and capacitor chip size A. Application examples are also discussed based on the proposed reliability model for Ni-BaTiO₃ MLCCs.

Introduction

Multilayer ceramic capacitors (MLCCs) are key building blocks in modern electronics [1]. MLCCs constitute ~30% of the total components in a typical hybrid circuit module such as a DC-DC converter. The numbers of ceramic capacitors used in integrated circuit (IC) power supply decoupling applications are even greater. Due to the increasing demand for decoupling capacitors and to the limited space available, the use of Ni-BaTiO₃ capacitors with a higher capacitance and a smaller chip size is more attractive for current large-scale IC chip packages.

Indeed, a typical central processing unit (CPU) package today requires more than 100 ceramic capacitors performing a variety of functions related to power delivery and signal integrity. These capacitors all need to work reliably for the CPU to function. Due to cost pressures, the degree of redundancy in CPU systems has been reduced, and so the failure of even one capacitor can cause the whole system to fail.

In its simplest form, capacitor system reliability can be expressed as:

$$Capacitor\ system\ reliability = component\ reliability^{\,Number\ of\ capacitors} \tag{1}$$

If a CPU system with 100 capacitors needs to maintain a system reliability of 99.9%, each capacitor must have an individual component reliability of 99.999% [2]. As a result, in order to improve system reliability, it is vital to better understand and improve the reliability of MLCCs.

Reliability of Ni-BaTiO₃ MLCCs

1. Reliability of MLCCs

The reliability of a MLCC is the ability of the dielectric material to retain its insulating properties under stated environmental and operational conditions for a specified period of time t. Reliability defects are the failures that might occur in the future inside a capacitor product that has been working well so far. Therefore, reliability must be regarded as a function of time and of external stresses. In addition, the construction and structural parameters of a MLCC device will also have an impact on its reliability.

To be presented by David (Donhang) Liu at the Capacitors and Resistors Technology Symposium (CARTS) conference, Santa Clara, California, April 1-3, 2014.

1

As a result, a general expression of MLCC reliability shall consist of three parts and can be expressed as [3]:

$$R(t) = \varphi(N, d, \bar{r}, A) \times AF(V, T) \times \gamma(t) \tag{2}$$

where: $\gamma(t)$ is a statistical distribution that describes the individual variation of properties in a testing group of samples (Weibull, log normal, normal, etc.); $AF(V,T)$ is an acceleration function that describes how a capacitor's reliability responds to external stresses such as applied voltage V and temperature T. All units in the testing group should follow the same acceleration function if they share the same failure mode (independent of individual units); and

$\varphi(N, d, \bar{r}, A)$ describes the effects on reliability from the structural and constructional characteristics of a capacitor device, such as the number of dielectric layers N, the dielectric thickness d, average grain size $\bar{r}$, and capacitor chip size A.

In general, a 2-parameter Weibull statistical distribution model is often used in the description of a Ni-BaTiO$_3$ capacitor's reliability as a function of time:

$$\gamma(t) = e^{-(\frac{t}{\eta})^{\beta}} \tag{3}$$

where e is the base for natural logarithms, β is the dimensionless *slope* parameter whose value is often characteristic of the particular failure mode under study, and η is the *scale* parameter that represents a characteristic time at which 63.2% of the population has failed and that is related to all other characteristic times, such as mean time to failure (MTTF):

$$MTTF = \eta \Gamma(1 + 1/\beta), \tag{4}$$

where $\Gamma(x)$ is the gamma function of x (Note: $\Gamma(1+1/\beta) \approx 0.9$ when $\beta > 3.0$).

Equation (3) provides a simple and clear understanding of the meaning of reliability:

- Reliability is a monotonic function of time and always decreases with time, which indicates that the loss of reliability is a common behavior for all devices.
- Since η and β always exceed zero, the value of $R(t)$ is always between 0 and 1, indicating that reliability can also be viewed as the probability of a failure occurring.
- Reliability typically defines the durability of a device that can function normally. When $\beta > 3$ and $t < \eta$, $R(t)$ ~1, suggesting a reliable lifespan before η. When t > η, $R(t)$ decreases rapidly to 0. The lifetime of a device to sustain its function can be characterized by η, as shown in Eq. (4).

2. Acceleration Functions of Ni-BaTiO$_3$ MLCCs

$AF(V,T)$ in the general reliability form of Eq. (2), represents the impacts of external stresses (applied voltage and temperature are commonly used) on the reliability of a Ni-BaTiO$_3$ capacitor. It is widely known that the time to failure (TTF) for a MLCC that is caused by a single failure mode when both V and T are changed from V_1 to V_2 and T_1 to T_2 is the product of the separate acceleration factors:

$$A_{VT} = \frac{t_1}{t_2} = \left(\frac{V_2}{V_1}\right)^n exp\left[\frac{E_a}{k}\left(\frac{1}{T_1} - \frac{1}{T_2}\right)\right] \tag{5}$$

where n is an empirical parameter that represents the voltage acceleration factors, E_a is an activation energy that represents the temperature acceleration factor, and k is the Boltzmann constant.

This well-known Prokopowicz and Vaskas equation has proven to be useful in the capacitor industry for testing MLCCs with precious metal electrodes (PMEs) at various highly accelerated testing conditions. An average of $n \approx 3$ has been found for the voltage acceleration factor, and an average value of $1 < E_a < 2$ eV is typical for the temperature acceleration factor [4].

To be presented by David (Donhang) Liu at the Capacitors and Resistors Technology Symposium (CARTS) conference, Santa Clara, California, April 1-3, 2014.

2

Since only a single failure mode is assumed, the value of β in Eq. (3) is usually assumed not to change with applied stresses. Only the Weibull distribution scale parameter η will change with external stresses. This can be expressed, according to Eq. (5), as

$$\eta(V,T) = \frac{C}{V^n} \cdot e^{\left(\frac{B}{T}\right)}, \tag{6}$$

where C and $B = E_a/k$ are constants.

Due to the impact of oxygen vacancy electromigration on the reliability of Ni-BaTiO$_3$ capacitors, the acceleration function $AF(V,T)$ of Ni-BaTiO$_3$ capacitors has been found to not always follow the power law with respect to applied voltage as specified in Eq. (5). Mixed failure modes have often been reported for Ni-BaTiO$_3$ capacitors [5-9].

A recent NASA-funded study that combines the measurement of both TTF and capacitor leakage current as a function of stress has been developed and used to describe the reliability of Ni-BaTiO$_3$ capacitors. A two-stage dielectric wear-out process that initiates with a slow dielectric degradation, followed by a thermally dominated catastrophic breakdown, has been revealed (Figure 1). When the failure criterion is set with respect to a leakage current level, some Ni-BaTiO$_3$ capacitors will reach the failure level with a catastrophic failure, and some will fail prior to the occurrence of a catastrophic dielectric breakdown [3, 8-9].
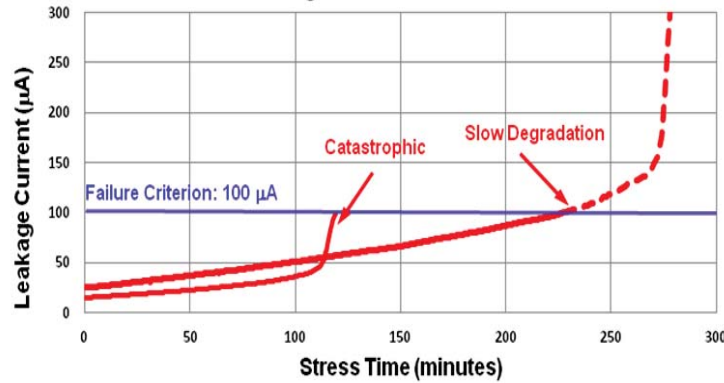

Figure 1. A two-stage dielectric wear-out failure mode is proposed to describe the dielectric breakdown behaviors in BME capacitors.

Further investigation also revealed that the two identified failure modes follow different acceleration functions. Slow degradation fits well to an exponential law against the applied field. Catastrophic failures fit the power-law better [3]. Table I summarizes the two failure modes and corresponding voltage acceleration functions that may be used to model the Ni-BaTiO$_3$ capacitors' reliability life.

Table I. Summary of Acceleration Functions for Ni-BaTiO$_3$ MLCCs

Failure mode	Acceleration function	Expression to scale parameter η	Expression to time to failure (TTF)
Slow Degradation	Exponential model	$\eta(E,T) = Ce^{-bE} \cdot e^{\left(\frac{E_a}{kT}\right)}$	$\frac{t_1}{t_2} = exp[-b(E_1 - E_2)]exp\left[\frac{E_a}{k}\left(\frac{1}{T_1} - \frac{1}{T_2}\right)\right]$
Catastrophic	Power-law (P-V equation)	$\eta(V,T) = \frac{C}{V^n} \cdot e^{\left(\frac{E_a}{kT}\right)}$	$\frac{t_1}{t_2} = \left(\frac{V_2}{V_1}\right)^n exp\left[\frac{E_a}{k}\left(\frac{1}{T_1} - \frac{1}{T_2}\right)\right]$

The Impact of Capacitor Structure on the Reliability of BME Capacitors

Ni-BaTiO$_3$ ceramic capacitors cannot be qualified for high reliability; they must be made for it. In other words, how a MLCC was designed, constructed, and processed will have a significant impact on the reliability of the final capacitor product. These parameters include the number of dielectric layers in a monolithic capacitor; the grain size, the dielectric layer thickness, or the combination of two; the number of grains per dielectric layer; and the chip size of a Ni-BaTiO$_3$ MLCC.

1. The Impact of the Number of Dielectric Layers

As shown in Figure 2, a monolithic MLCC can be converted both constructively and electrically to a number of single-layer ceramic capacitors connected in parallel. Assuming C_i is the i-th layer capacitor, the MLCC can be viewed as a parallel connection among $C_1, C_2, C_3, \ldots C_i, \ldots$, and C_N, where N the number of dielectric layers inside a MLCC device. Since every single-layer capacitor C_i shares the same electrode area S, the same dielectric thickness d, and the same processing history, it is reasonable to assume that $C_1 = C_2 = C_3 = \cdots = C_i \ldots = C_N$.

So the sum of the capacitance C_t of a MLCC can be expressed as:

$$C_t = C_1 + C_2 + C_3 \ldots + C_i \ldots + C_N = N \cdot C_i. \tag{7}$$

Similarly, the reliability of a MLCC with N dielectric layers that are connected in parallel can be expressed as:

$$R_t = R_1 \times R_2 \times R_3 \ldots \times R_i \ldots \times R_N = R_i^N, \tag{8}$$

where R_i is the reliability of an i-th single-layer capacitor, and R_t is the overall reliability of a MLCC.
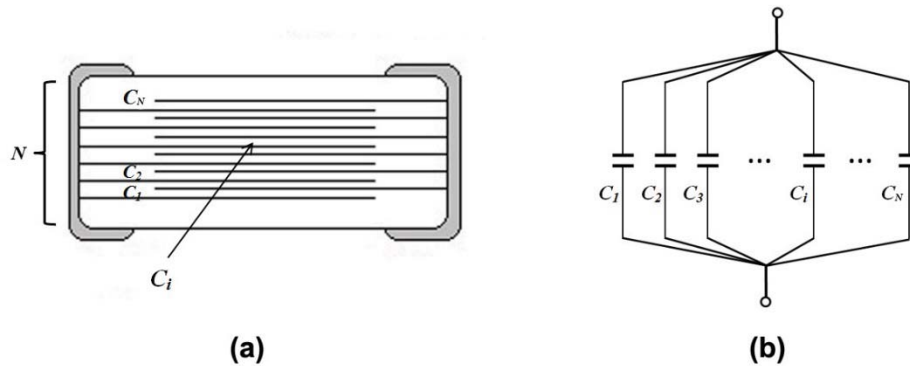

Figure 2. A cross-sectional view of a monolithic MLCC shows a stack of N layers of single-layer capacitors (a); this construction can be equivalently converted to the same number of single-layer capacitors connected in parallel.

The reliability relationship shown in Eq. (8) indicates that the overall reliability R_t of a MLCC device is highly dependent on the reliability R_i of a single-layer capacitor inside a monolithic MLCC body.

From the structure of a MLCC unit shown in Figure 2, capacitor reliability can be expressed as:

$$R_t(t) = R_i(t)^N \tag{9}$$

where N is the number of individual dielectric layers and $R_i(t)$ is the reliability of a dielectric layer. The capacitor reliability $R_t(t)$ as a function of $R_i(t)$ and N is shown in Figure 3.

In general, when dielectric reliability $R_i(t)$ is very close to unity, N does not have a significant impact on MLCC reliability $R_t(t)$. If $R_i(t)$ is reduced slightly, the overall reliability $R_t(t)$ of a MLCC can degrade rapidly due to the amplifying effect of the number of dielectric layers N. Since most commercial Ni-BaTiO$_3$ capacitors are made with a large number of dielectric layers (typically $N > 250$), the impact of N on Ni-BaTiO$_3$ capacitor reliability is critical.
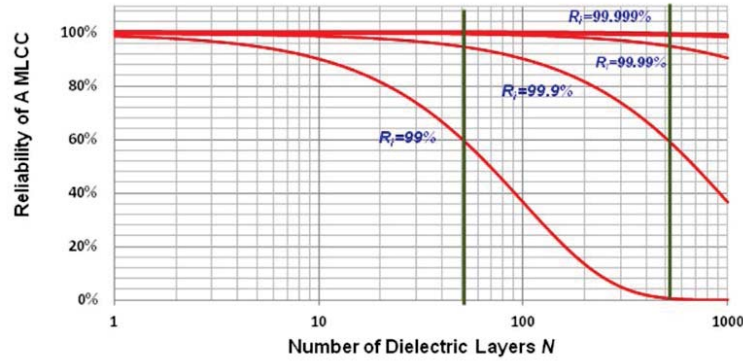
Figure 3. MLCC reliability $R_t(t)$ as a function of dielectric reliability $R_i(t)$ and number of dielectric layers N.

2. The Impact of Number of Grains per Dielectric Layer

As shown in Figure 4, if a single-layer capacitor C_i has an average grain size $\bar{r}$ and an average dielectric thickness d, the number of grains per dielectric layer can be calculated as $\left(\frac{d}{\bar{r}}\right)$.
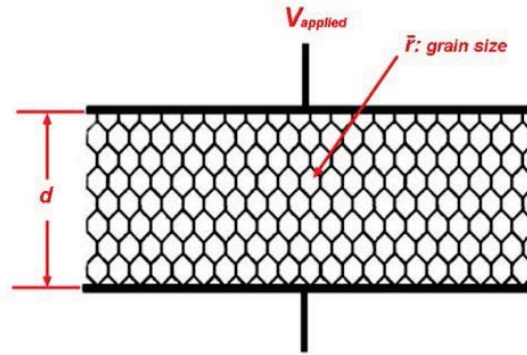

Figure 4. Estimate of the number of grains in a dielectric layer. With average dielectric thickness d and average grain size $\bar{r}$, the number of grains per dielectric layer can be calculated as $\left(\frac{d}{\bar{r}}\right)$.

The MTTF of Ni-BaTiO$_3$ MLCCs as a function of parameter $\left(\frac{d}{\bar{r}}\right)$ was measured and reported recently at high temperature (150°C) and high DC field (10kV/mm) by a Ni-BaTiO$_3$ capacitor manufacturer [10]. The measured MTTF data were found to be proportional to the number of grains $\left(\frac{d}{\bar{r}}\right)$. But if the voltage-per-grain-boundary is adjusted to the same value, all MLCCs under test with different $\left(\frac{d}{\bar{r}}\right)$ values give rise to almost identical MTTF values. According to Eqs. (5) and (6), the MTTF of a Ni-BaTiO$_3$ capacitor at a given temperature can be directly written as:

$$MTTF = \frac{1}{V_{grain}^{n}} = \frac{1}{\left[\frac{V_{applied}}{\left(\frac{d}{\bar{r}}\right)}\right]^{n}} = \frac{1}{V_{applied}^{n}} \times \left(\frac{d}{\bar{r}}\right)^{n}. \tag{10}$$

This indicates that the MTTF of Ni-BaTiO$_3$ capacitors follow a power-law relationship for the dielectric thickness d when applied voltage and average grain size are both given.

In order to implement the microstructure parameter $\left(\frac{d}{\bar{r}}\right)$ into the reliability of a single-layer capacitor, a structural model based on the dielectric thickness and the feature size of a defect can be developed.

To be presented by David (Donhang) Liu at the Capacitors and Resistors Technology Symposium (CARTS) conference, Santa Clara, California, April 1-3, 2014.

5

As shown in Figure 5, assuming that the feature size of a defect that causes a catastrophic failure is r, d is the dielectric thickness, and the reliability of the defect is 0, then the reliability of a single dielectric layer $R_i(t)$ with thickness d will be determined by the value of d with respect to r. When d is far greater than the defect feature size r, the defect is non-harmful and may not cause any failures for many years, or even during a capacitor's lifetime.
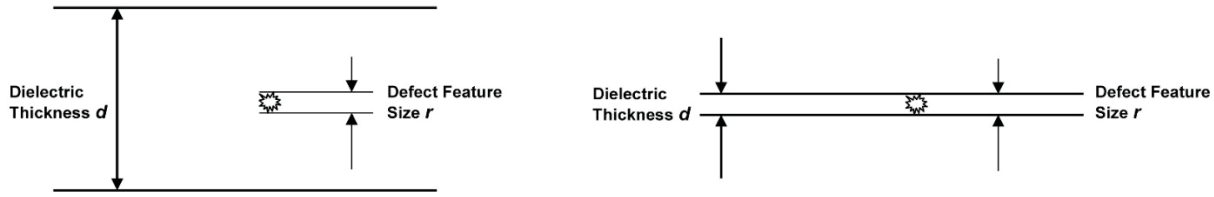

Figure 5. An illustration of dielectric thickness d with respect to feature size r of an extrinsic defect inside the dielectric layer. The dielectric layer reliability is dependent on the ratio r/d:

(a): $d >> r$; (b): $d \approx r$.

However, as d approaches the feature size of the defect r, the defect will cause dielectric failure instantly. In other words, the survival probability of the dielectric layer R_i can be written as $R_i(t) \rightarrow 1$ when $d >> r$ and as $R_i(t) \rightarrow 0$ when $d \approx r$. According to Eq. (10), the Weibull reliability of a dielectric layer with respect to its thickness d and defect feature size r can thus be expressed as:

$$R_i(t) = e^{-\left(\frac{t}{\eta}\right)^{\beta}} \cdot \left[1 - \left(\frac{r}{d}\right)^{\xi}\right].$$

For simplicity, the defect size r can be directly related to the average grain size $\bar{r}$ as: $r \approx c \times \bar{r}$, where c is a constant. The equation above can be further expressed with respect to average grain size $\bar{r}$ as:

$$P = \left[1 - \left(\frac{r}{d}\right)^{\xi}\right] = \left[1 - \left(\frac{\bar{r}}{d}\right)^{\alpha}\right], \quad (\alpha \geq 5) \tag{11}$$

where P is a geometric factor that determines the dielectric layer reliability $R_i(t)$ with respect to the microstructure of a MLCC. α is an experimental constant that was determined by the formulation, processing conditions, and microstructure of a BME capacitor. α was experimentally determined in this study such that $\alpha \approx 6$ for V ≤ 50 V and $\alpha \approx 5$ for V > 50 V.

The Weibull reliability of a Ni-BaTiO$_3$ capacitor is equal to unity when $t < \eta$, so the reliability of a single dielectric layer inside of a MLCC can be expressed as:

$$R_i(t < \eta) = e^{-\left(\frac{t}{\eta}\right)^{\beta}} \cdot \left[1 - \left(\frac{\bar{r}}{d}\right)^{\alpha}\right] = 1 \cdot \left[1 - \left(\frac{\bar{r}}{d}\right)^{\alpha}\right] = \left[1 - \left(\frac{\bar{r}}{d}\right)^{\alpha}\right].$$

Combining Eqs. (9) and (11) yields the time-independent, simplified reliability of a BME MLCC:

$$R_t(t < \eta) = R_i(t < \eta)^N = \left[1 - \left(\frac{\bar{r}}{d}\right)^{\alpha}\right]^N, \quad (\alpha \geq 5). \tag{12}$$

Eq. (12) shows that a reliability defect may function in two different ways when it exists in a single-layer capacitor. Such a defect can be benign for the rest of the product life without causing a failure if the feature size of the reliability defect is much less than that of the dielectric thickness. On the other hand, the defect may cause catastrophic failures if the feature size approaches that of the dielectric thickness and if the level of external stress is extremely high.

To be presented by David (Donhang) Liu at the Capacitors and Resistors Technology Symposium (CARTS) conference, Santa Clara, California, April 1-3, 2014.

6

3. The Impact of Capacitor Chip Size A

In order to reveal the impact of chip size on the reliability of BME MLCCs, the effective areas of MLCC devices with different chip sizes were measured and normalized with respect to the Electronic Industries Alliance (EIA) chip size of 0402, the smallest chip size used in this comparison study. Corresponding measured results are summarized in Table II. The chip size scaling factor S represents how many times larger the effective area of a given EIA chip size is than that of 0402 for a single dielectric layer. For example, the effective chip size of a 0805 MLCC is equal to 6.76 times that of a 0402 MLCC connected in parallel.

Per Figure 2, Table II, and Eq. (9), the single dielectric layer reliability of a 0805 MLCC $R_i(0805)$ can be expressed with respect to that of a 0402 MLCC $R_i(0402)$ as:

$$R_i(0805) = R_i(0402)^{6.76}.$$

Table II. EIA Chip Size and Calculated Scaling Factors for BME Capacitors

Chip size	Length (μm)	Width (μm)	Terminal-t (μm)	Side margin (μm)	End margin (μm)	Effective area of a single dielectric layer (mm^2)	Chip size scaling factor s
0402	1000 ± 100	500 ± 100	250 ± 150	125	100	0.225	1.00
0603	1600 ± 150	810 ± 150	350 ± 150	175	100	0.763	3.39
0805	2010 ± 200	1250 ± 200	500 ± 200	250	150	1.520	6.76
1206	3200 ± 200	1600 ± 200	500 ± 200	250	150	3.510	15.60
1210	3200 ± 200	2500 ± 200	500 ± 200	250	150	5.940	26.40
1812	4500 ± 300	3200 ± 200	610 ± 300	300	200	10.920	48.53
2220	5700 ± 400	5000 ± 400	640 ± 390	320	220	23.074	102.55
1825	4500 ± 300	6400 ± 400	610 ± 360	300	220	23.244	103.31

In general, when the chip size scaling factor S is used, the single dielectric layer reliability of a MLCC with an EIA chip size of xy can be expressed with respect to the single dielectric layer reliability of a 0402 MLCC as:

$$R_i(xy) = R_i(0402)^s. \tag{13}$$

When the chip size scaling factor increases by a hundredfold, the single dielectric layer reliability declines: 45% when $R_i(0402)= 99\%$; 10% when $R_i(0402)= 99.9\%$; and 1% when $R_i(0402)= 99.99\%$. The single dielectric layer reliability of MLCCs decreases with increasing chip size, but not significantly in comparison to the reliability decrease that accompanies an increase in the number of dielectric layers. Results are shown in Figure 6.

Furthermore, according to Eq. (9), the reliability of a MLCC with chip size xy $R_t(xy)$ can be expressed as:

$$R_t(xy) = [R_i(0402)^{N_{xy}}]^s = \left[R_t(0402)^{\frac{N_{xy}}{N_{0402}}} \right]^s, \tag{14}$$

where $R_t(xy)$ is the reliability of a BME MLCC with a chip size of xy and N_{xy} of dielectric layers, and $R_t(0402) = R_i(0402)^{N_{0402}}$ is that with a 0402 chip size and N_{0402} of dielectric layers. Construction analysis of Ni-BaTiO$_3$ capacitors has revealed that $N_{0402} \approx 70$–80 and $N_{xy} \approx 250$–300, so that $\frac{N_{xy}}{N_{0402}} \approx 3$–$4$.

To be presented by David (Donhang) Liu at the Capacitors and Resistors Technology Symposium (CARTS) conference, Santa Clara, California, April 1-3, 2014.
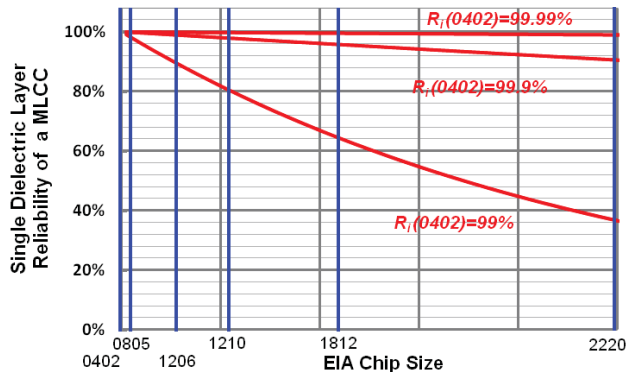
7

Figure 6. The single dielectric layer reliability R_i (xy) as a function of EIA chip size, and the single layer reliability of a 0402 MLCC R_i (0402).

Conversely, the dielectric thickness of Ni-BaTiO$_3$ capacitors is also found to gradually increase with MLCC chip size A. Figure 7 shows construction analysis results of average Ni-BaTiO$_3$ dielectric thickness as a function of chip size. According to Eq. (10), the MTTF of a MLCC follows a power-law increase with increasing dielectric thickness. Therefore, the reliability decreases due to increasing chip size have been greatly compensated for by increasing the dielectric thickness.

As a result of that, the overall reliability of a Ni-BaTiO$_3$ MLCC will not change significantly with increasing capacitor chip size.
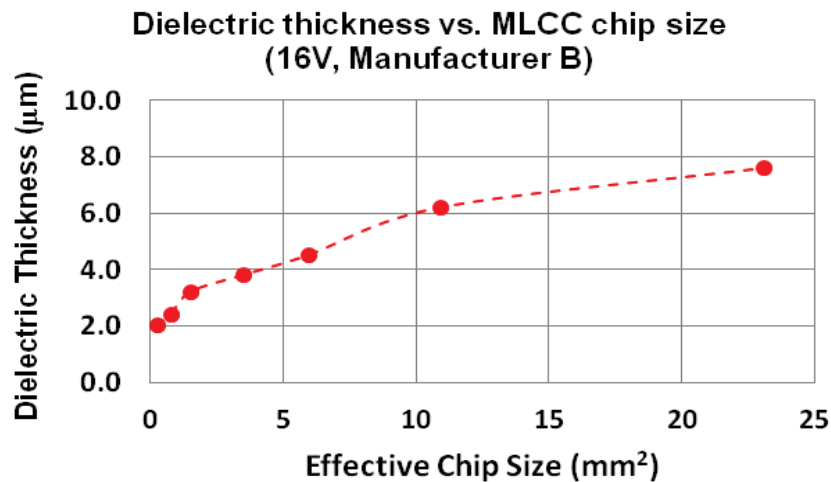

Figure 7. Measured average dielectric thickness as function of BME MLCC chip size A.

To be presented by David (Donhang) Liu at the Capacitors and Resistors Technology Symposium (CARTS) conference, Santa Clara, California, April 1-3, 2014.

8

Application Examples

The general expression of a BME capacitor's reliability as given in Eq. (2) can be specifically rewritten for Ni-BaTiO$_3$ capacitors based on this study. A two-parameter Weibull distribution is applicable to $\gamma(t)$. Two identified failure modes will follow different acceleration functions $AF(V,T)$, as summarized in Table I. Function $\varphi(N, d, \bar{r}, A)$ can be expressed using Eq. (12). The impact of chip size S on the reliability of BME capacitors is negligible. Therefore, the reliability of a Ni-BaTiO$_3$ capacitor is finally obtained:

$$R(t) = \varphi(N, d, \bar{r}, A) \times AF(V,T) \times \gamma(t)$$

$$= \left[1 - \left(\frac{\bar{r}}{d}\right)^{\alpha}\right]^{N} \times \left\{ p \times e^{-\left[\frac{t}{\frac{a}{V^n}\cdot e^{\left(\frac{E_{a1}}{kT}\right)}}\right]^{\beta_1}} + (1-p) \times e^{-\left[\frac{t}{Ce^{-bE}\cdot e^{\left(\frac{E_{a2}}{kT}\right)}}\right]^{\beta_2}} \right\}, \qquad (15)$$

where β_1 and β_2 are the Weibull slope parameters for catastrophic and slow degradation failures, respectively; E_{a1} and E_{a2} are the activation energies for the two failure modes, respectively; p is the percentage of catastrophic failures; a, b, C are constants; α is a constant that can be determined experimentally; and N, d, and $\bar{r}$ are the number of dielectric layers, average dielectric thickness, and average grain size, respectively.

1. Reliability Model at *t=0*

From Eq. (15), when *t*=0, the general reliability model is simplified to a constant that is only dependent on the structural and construction parameters of a MLCC device.

$$R(0) = \left[1 - \left(\frac{\bar{r}}{d}\right)^{\alpha}\right]^{N}.$$

Table III summarizes the calculated *R(0)* data for a number of commercial Ni-BaTiO$_3$ MLCCs based on the construction analysis results. It has been found that when Eq. (16) is satisfied, most Ni-BaTiO$_3$ MLCCs pass 1000-hour life testing at 125°C and twice the rated voltage specified in MIL-PRF-55681.

Table III. Calculated Reliability Data per Eq. (16) and Corresponding Life Test Results

CAP ID	Grain Size (µm)	Dielectric Thickness(µm)	No. of Dielectric Layers N	Calculated *R(0)*	1000-hours Life Test at 125°C, 2 x Vr
A08X22525	0.305	3.89	211	0.99995	Fail
B08X33425	0.420	5.80	74	0.99999	Pass
A08X15425	0.460	9.80	43	1.00000	Pass
C06X10525	0.440	3.20	150	0.99899	Fail
A06X10425	0.470	7.89	62	1.00000	Pass
A12X47425	0.492	10.40	58	1.00000	Pass
C04X47325	0.386	4.40	60	0.99997	Fail
B12X47525	0.376	4.34	260	0.99989	Fail
P08X10425	0.790	20.20	23	1.00000	Pass
B06X10516	0.273	2.29	179	0.99948	Fail
A08X47416	0.319	3.75	208	0.99992	Fail
B12X68416	0.375	6.21	64	1.00000	Pass
C08X22516	0.224	3.81	212	0.99999	Pass
B08X22516	0.340	3.23	230	0.99969	Fail
B08X56416	0.373	4.21	80	0.99996	Pass
C08X47516	0.230	2.49	260	0.99984	Pass

B12X10516	0.475	7.82	99	1.00000	Pass
B04X10416	0.342	3.05	67	0.99987	Fail
B12X10606	0.365	3.11	348	0.99908	Fail
B04X10406	0.323	2.50	70	0.99967	Fail
B08X22506	0.419	3.42	230	0.99922	Fail
A08X10406	0.490	12.50	34	1.00000	Pass
B06X22406	0.373	4.01	67	0.99996	Pass
P06X10405	0.770	12.60	24	1.00000	Pass

*: Capacitor ID: C (manufacturer ID); 08 (EIA chip size, 08=0805); X (dielectric type, X=X7R); 475 (cap values, 475=4,700,000 pF); 16 (rated voltage). For example: A08X10406 = 100,000pF, 6V, 0805, from manufacturer A.

In addition, all of the commercially available automotive-grade Ni-BaTiO$_3$ MLCCs (that meet the requirements of AEC-Q200) that have been processed for construction and microstructure investigations have been found to meet the conditions of Eq. (16).

$$R(0) = \left[1 - \left(\frac{\bar{r}}{d}\right)^{\alpha}\right]^{N} = 1.00000. \tag{16}$$

One may wonder why there must be 5 zeroes in Eq. (16). As discussed previously, BX% is a better term over MTTF to describe the reliability life of Ni-BaTiO$_3$ MLCCs [3]. When predicting reliability life, it is important to know the rate at which a population will fail. To better predict the reliability life of Ni-BaTiO$_3$ capacitors, it is preferable that BX% life be used.

BX% refers to the time by which *X%* of the units in a population will have failed. BX% life of a *2*-parameter Weibull can be calculated using Eq. (17). The BX% life is not only related to the model parameters but is also directly related to the reliability $R(t)$ that is a function of time.

$$t_R = \eta \cdot \{-ln[R(t_R)]\}^{1/\beta} \tag{17}$$

where $R(t_R) = 1\text{-}X\%$, which corresponds to the probability that *1-X%* units in the population have not failed at t_R.

According to MIL-PRF-55681, the reliability level of a MLCC is defined by 1000 hours at a given failure rate level. Table IV summarizes the reliability levels per MIL-PRF-55681 and the corresponding calculated BX% life at different failure rates. It is clear that the number of zeroes in Eq. (16) corresponds to the reliability life of a level *S*, or a 1000-hour lifetime with a failure rate of 100 ppm (parts per million).

Table IV. Product Level in MIL-PRF-55681 and Corresponding Calculated BX% Life with Respect to the Failure Rate for MLCCs

Product level per MIL-PRF-55681		BX% life and reliability level per Eq. (17)	
Symbol	Failure rate level (%) (percent per 1000 hours)	BX% life (hours) to failure rate	BX% life to reliability
M	1.0	BX1.0%=1000	R(1.0%)=0.99
P	0.1	BX0.1%=1000	R(0.1%)=0.999
R	0.01	BX0.01%=1000	R(0.01%)=0.9999
S	0.001	BX0.001% =1000	R(0.001%)=0.99999

Although a significant amount of Ni-BaTiO$_3$ MLCCs that meet Eq. (16) have passed the life test at 125°C and twice the rated voltage for 1000 hours, Eq. (16) is not sufficient to be used to predict the reliability life of Ni-BaTiO$_3$ MLCCs. Indeed, for users of Ni-BaTiO$_3$ MLCCs, Eq. (16) can be used as a selection criterion for Ni-BaTiO$_3$ MLCCs that can be considered for high-reliability applications because most of the Ni-BaTiO$_3$ MLCCs that meet Eq. (16) can pass the life test per MIL-PRF-55681. Those that do not meet this requirement can be rejected prior to tedious life testing, thus saving time and effort.

For manufacturers, Eq. (16) can be used as a simple rule of thumb when designing Ni-BaTiO$_3$ MLCCs for high-reliability applications. However, it should be pointed out that since some dopants used in formulating Ni-BaTiO$_3$ MLCCs, such as Ca and Mg, may function as grain growth prohibiters, tone must be very careful when using Eq. (16) to compare Ni-BaTiO$_3$ MLCCs. It is recommended that only Ni-BaTiO$_3$ MLCCs with similar formulations and processing conditions should be compared using Eq. (16). It is also worth mentioning that per Eq. (16), at a given dielectric thickness and number of dielectric layers, the smaller grain size would give rise to a better reliability.

2. Reliability Model at t>0

When $t > 0$, Eq. (15) suggests two different failure modes in Ni-BaTiO$_3$ MLCCs that follow different acceleration functions with external applied stress. Figure 8 shows a number of TTF data sets obtained for a Ni-BaTiO$_3$ MLCC of C08X47516 at various stress conditions during highly accelerated life stress testing (HALST), in which a data set obtained at 135°C and 72V is used for model verification purposes only. This data set will not be used in statistical modeling to determine the acceleration factors; it will only be used to compare the calculated MTTF results from Weibull modeling.

All TTF data sets appear to fit to single Weibull plots, indicating a single failure mode. When the Prokopowicz and Vaskas equation (Eq. (5)) is used to process the Weibull modeling data shown in Figure 8, the acceleration factors E_a and n can be determined. The Weibull reliability life as characterized by MTTF can then be calculated for various stress conditions.
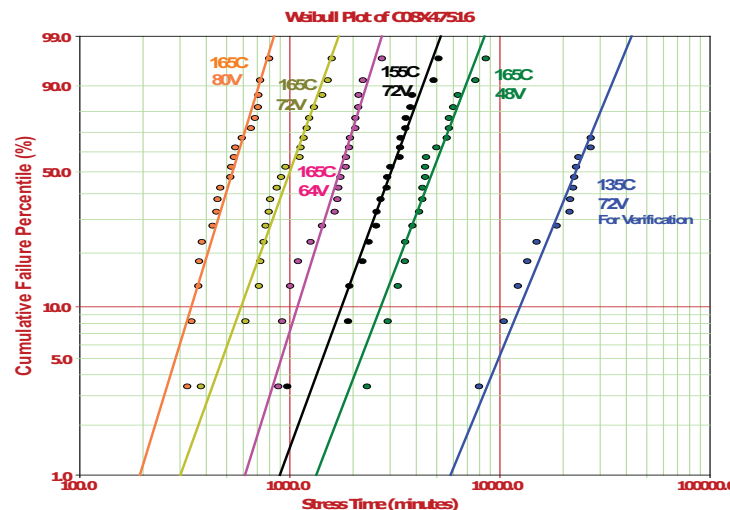

Figure 8. Weibull plots of a number of TTF data under various stress conditions. The MTTF, β, and η values are also included for information. The TTF data that were obtained at 135°C, 72V are for verification of the model only and were not used for the reliability modeling.

Table V summarizes the calculated MTTF and compares it to experimentally determined MTTF data at 135°C, 72V. It is clear that the calculated lifetime of 2111.17 hours is much longer than the 318.28 hours actually measured. Indeed, the inconsistency between calculated MTTF using a single Weibull model and Eq. (5) and that of actual measured MTTF has been observed for quite a while for many Ni-BaTiO$_3$ MLCCs. Calculated lifetimes often have been found to be longer than measured ones [1].

Table V. Calculated Statistical Parameters and Acceleration Factors for a Ni-BaTiO$_3$ Capacitor C08X47516

	Acceleration Factors from P-V Equation and MTTF Calculated for 135°C, 72V					
Weibull Model Parameters	β	η	E_a (eV)	n	MTTF (min)	MTTF (Hours)
Calculated Data	2.755	3.587E+07	2.60	4.524	126670.20	2111.17
Verification Data at 135°C, 72V	3.822	21124	N/A	N/A	19097.00	318.28

As has been suggested before [3, 8-9], this inconsistency is likely due to the existence of mixed failure modes. Since the traditional highly accelerated life test is a method that is based on a single failure mode, it is necessary to introduce another independent test parameter, in addition to TTF, to reveal the complexity of failure modes in Ni-BaTiO$_3$ MLCCs. In this study, leakage current as a function of applied stress time was measured together with TTF data. Figure 9 shows corresponding leakage current data at a stress condition of 165°C and 72V, together with the TTF data shown in Figure 8. It is clear that the measured leakage current data reveal two distinct failure modes: (a) a catastrophic failure, characterized by a gradual leakage increase followed by a time-accelerating increase in leakage, and (b) a slow degradation, characterized by a near-linear leakage increase until the failure criterion is reached.

Figure 10 shows a re-plot of the Weibull probability plots of the TTF data shown in Figure 9 with respect to the failure modes. Arrows are used to indicate the data points that failed catastrophically. Corresponding failure modes for each TTF data points in the plot are listed in the chart on the right-hand side of Figure 10.

Weibull modeling of the data shown in Figure 10 was performed as follows: When all of the catastrophic data points were processed as failures, the others in the group were treated as suspensions. The process was switched, with all slow degradation failures processed as failures and all catastrophic ones treated as suspensions. As a result, the original mixed TTF data set could be separated into "catastrophic" and "slow degradation" subsets that were modeled separately. Figure 11(a) shows the Weibull plots from two subsets as distinguished in Figure 10.
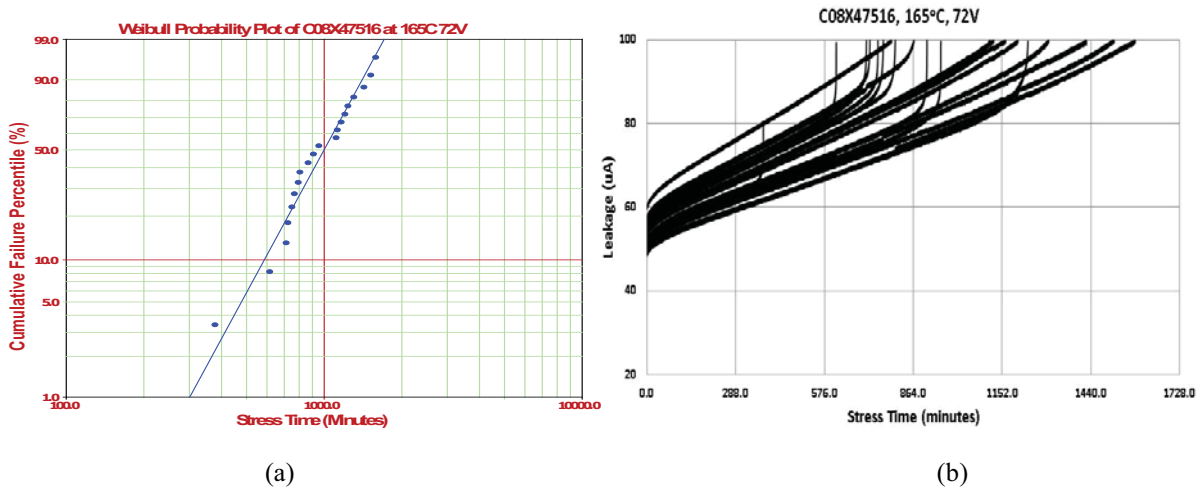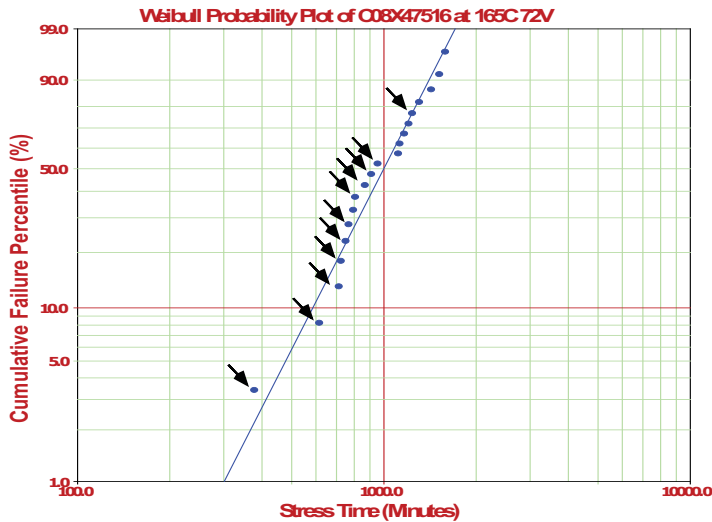

(a)   (b)

Figure 9. The Weibull plot of TTF data and corresponding leakage current measurement results are shown together. The leakage current data are characterized by mixed failure modes that are not revealed in the corresponding TTF measurement.

TTF (minutes)	Failure Mode	symbol
377.26	Catastrophic	C
614.70	Catastrophic	C
712.00	Catastrophic	C
723.40	Catastrophic	C
749.30	Catastrophic	C
766.34	Catastrophic	C
793.25	Slow Degradation	S
805.29	Catastrophic	C
866.30	Catastrophic	C
908.27	Catastrophic	C
953.18	Catastrophic	C
1112.39	Slow Degradation	S
1124.51	Slow Degradation	S
1163.47	Slow Degradation	S
1203.19	Slow Degradation	S
1235.54	Catastrophic	C
1302.47	Slow Degradation	S
1425.38	Slow Degradation	S
1515.23	Slow Degradation	S
1583.30	Slow Degradation	S

Figure 10. A re-plot of Weibull modeling as shown in Figure 9, with arrows indicating the catastrophic failures when the leakage current data were applied to distinguish between the two different failure modes.

Corresponding contour plots of the two subsets are shown in Figure 11(b). A contour plot gives rise to a visual picture of confidence bounds on β and η for a *2*-parameter Weibull distribution at a certain confidence level (typically 95%). The plot defines the boundary of a data set with respect to the possible values of β and η, and it is often applied to compare different data sets for different failure modes and to determine whether two sets have statistically different failure modes.

It is important to note that in the contour plots shown in Figure 11(b), the two data sets do not show any overlap with respect to the β values (*Y*-axis). This is a clear indication that the two data sets statistically represent two different failure modes, as characterized by two different β values.

What makes this example even more interesting is the fact that the TTF data shown in Figure 9(a) would appear to fit a single Weibull model well (a linear-like curve) if the leakage current data shown in Figure 9(b) were not used. However, when the leakage current data are used to distinguish the failure modes, the TTF data that seem to fit a single failure mode can clearly be separated into two subsets with two different β values, indicating that the two subsets have different failure modes.
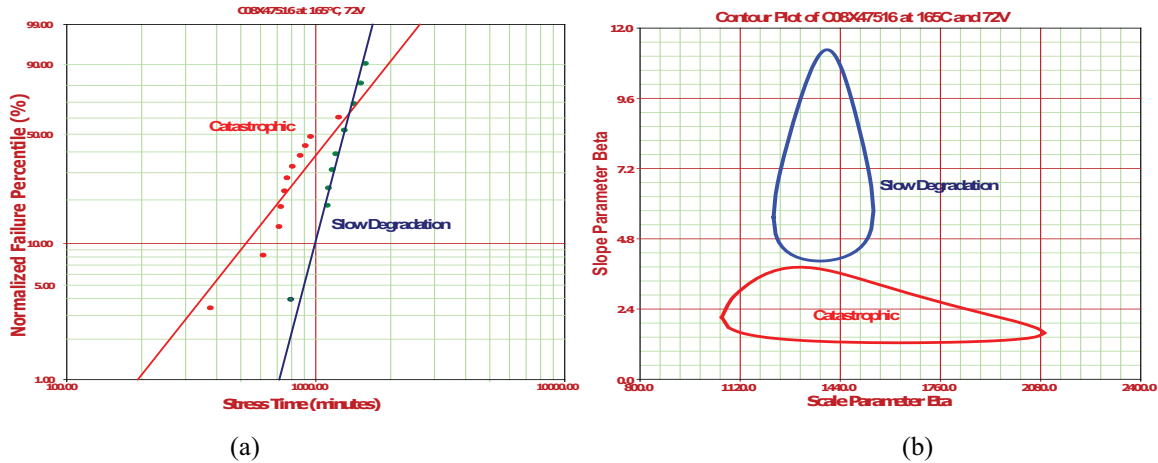
Figure 11. Weibull modeling plots using the TTF data and failure modes information revealed in Table II from the corresponding leakage current measurement (a). Contour plot reveals the two slope parameters β for the two different failure modes, but the two subgroups share a similar scale parameter η (b).

To repeat the process shown in Figures 9 and 10 for all data sets shown in Figure 8, the data sets can be split into two separate subsets with two different failure modes. The normalized Weibull probability plots at 125°C and 32V (twice the rated voltage) are shown in Figure 12(b) for three different failure scenarios, in which each data point is extrapolated from Figure 12(a) using a most likelihood estimation (MLE) method and a power-law acceleration function for catastrophic failures and an exponential-law acceleration function for slow degradation failures (Table I). This is done for each failure and for any suspensions that are entered, and then the median ranks of the failures are determined. Additional details on this approach for characterizing HALST results have been described previously [8, 9].

A total of three normalized Weibull plots were generated to represent the two distinct failure modes that were revealed in leakage current measurements, as well as a mixture of both. The plot labeled "complete set" is the normalized Weibull plot that all TTF data points shown in Figure 12(a) were used for modeling, except the data set of 135°C, 72V. This plot also represents a conventional Weibull plot when all of the units are assumed to fail with only a single failure mode. The "catastrophic" plot is created using all of the data points that failed with a catastrophic characteristic and with all remaining data points (that failed with slow degradation) set as suspensions. The "slow degradation" plot is one in which only slow degradation failed samples were used for Weibull modeling and those that failed catastrophically remain suspensions.

It is noticeable that the three Weibull modeling plots give rise to different scale parameters η, indicating that each model predicts a different reliability life. The calculated MTTF for the catastrophic failure mode with power-law acceleration function (Eq. (5)) at 135°C, 72V is 318.7 hours, which is almost identical to the MTTF value of 318.3 hours estimated from the data set of 135°C, 72V shown in Figure 12(a). In addition, the leakage current measurement also showed that all data points for 135°C, 72V revealed a catastrophic failure mode [3].
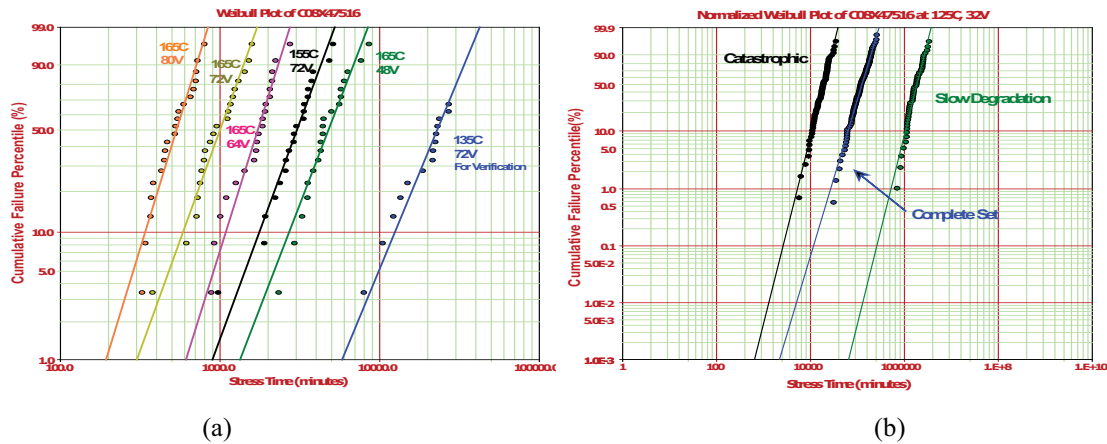
Figure 12. Weibull plots for BME capacitor C08X47516 under various stress conditions (a); corresponding normalized probability plots at 125°C and 32V, with a power-law acceleration factor (b).

Summary

A general reliability model for Ni-BaTiO$_3$ MLCCs has been proposed and verified. The model consists of three parts: (1) a 2-parameter Weibull distribution; (2) two acceleration functions that describe two statistically distinct failure modes: a power-law form for catastrophic failures, and an exponential-law form for slow degradation failures; (3) an empirical function that defines contribution of the structural and constructional characteristics of a multilayer capacitor device, such as the number of dielectric layers N, dielectric thickness d, and average grain size $\bar{r}$. The capacitor chip size A is found not to play a role in the reliability of a Ni-BaTiO$_3$ MLCC.

Two examples are discussed for the application of this reliability model. At $t=0$, the reliability model can be used as a selection criterion for Ni-BaTiO$_3$ MLCCs that may be applicable to high-reliability applications. When $t>0$, the proposed reliability model defines two distinct failure modes in Ni-BaTiO$_3$ MLCCs. The calculated reliability life using the proposed model gives rise to a good agreement with measured MTTF results.

Acknowledgements

References

[1] H. Kishi, Y. Mizono, H. Chazuno, H. Chazono , *Jpn. J. Appl. Phys.* Vol. 42, p. 1, 2003
[2] C. Hendricks, Y. Min, T. Lane, and V. Magadala, *CARTS Proceedings,* New Orleans, LA,p. 3, 2010
[3] D. Liu, *CARTS Proceedings,* Houston, TX, p. 235, March 2013
[4] T. I. Prokopowicz and A. R. Vaskas, Final Report ECOM-90705-F, NTIS AD-864068, October 1969
[5] B. Rawal and N. Chan, *Proceedings of Electronic Components Conference*, New Orleans, p. 184, 1984
[6] J. L. Paulsen and E. K. Reed, *Microelectronics Reliability,* Vol. 42, p. 815, 2002
[7] M. Randall, A. Gurav, D. Skamser, and J. Beeson, *CARTS Proceedings*, p. 134, 2003
[8] D. Liu and M. Sampson, *CARTS Proceedings*, Jacksonville, FL, p. 45, 2011
[9] D. Liu and M. Sampson, *CARTS Proceedings*, Las Vegas, NV, p. 59, 2012
[10] T. Nakamura, T. Yao, J. Ikeda, N. Kubodera, H. Takagi, *IOP Conf. Series: Materials Science and Engineering* Vol. 18, p. 1, 2011